Magnetic anisotropy and metamagnetic behaviour of the bimetallic chain $MnNi(NO_2)_4(en)_2$ (en = ethylenediamine)

2001 J. Phys.: Condens. Matter 13 2639

(http://iopscience.iop.org/0953-8984/13/11/319)

INSTITUTE OF PHYSICS PUBLISHING JOURNAL OF PHYSICS: CONDENSED MATTER

J. Phys.: Condens. Matter **13** (2001) 2639–2650 www.iop.org/Journals/cm PII: S0953-8984(01)17381-9

Magnetic anisotropy and metamagnetic behaviour of the bimetallic chain $MnNi(NO_2)_4(en)_2$ (en = ethylenediamine)

R Feyerherm[1,3], C Mathonière[2] and O Kahn[2]

[1] Hahn–Meitner Institute GmbH, 14109 Berlin, Germany
[2] Institut de Chimie de la Matière Condensée de Bordeaux, ICMCB, 33608 Pessac, France

E-mail: feyerherm@hmi.de

Received 22 September 2000, in final form 31 January 2001

Abstract

Single-crystal magnetization, heat capacity and neutron diffraction studies of the bimetallic regular chain $Mn^{II}Ni^{II}(NO_2)_4(en)_2$ (en = ethylenediamine) are presented. This compound exhibits ferromagnetic interactions between the Mn and Ni ions within the chains. The onset of long-range antiferromagnetic ordering below $T_N = 2.45$ K is associated with weaker antiferromagnetic interactions between neighbouring chains. The magnetization studies reveal an easy axis anisotropy of the susceptibility at low T with a preferred orientation $\| c$. This anisotropy results from the low local symmetry around the Mn ions. Below T_N, the susceptibility drop observed for $H \| c$ is much larger than for $H \perp c$, pointing to a moment orientation parallel to the c axis in the ordered state. At 1.8 K, the metamagnetic transition is observed to proceed in two steps for $H \| c$, with $H_{c1} = 1.5$ kOe and $H_{c2} = 2.5$ kOe. This is associated with the familiar spin flop state at the intermediate field values. For $H \perp c$, at 1.8 K the ordered state is suppressed only in fields larger than 6 kOe. Low-T heat capacity data exhibit a pronounced anomaly at the antiferromagnetic transition. The reduced entropy at T_N points to significant short-range ordering effects above T_N associated with the ferromagnetic intrachain interactions. The ordered magnetic structure is an antiferromagnetic stacking of ferromagnetic sheets.

1. Introduction

Chain compounds of magnetic ions have attracted the interest of chemists and physicists for more than three decades. Bimetallic chains, in which two types of metal ion alternate, are of specific interest [1–4]. In general, in these compounds the two metal species are antiferromagnetically coupled but their magnetic moments do not compensate, resulting in one-dimensional ferrimagnetic behaviour. In the presence of interchain interactions, long-range

[3] Full address of corresponding author: Dr Ralf Feyerherm, Hahn–Meitner Institute, Glienicker Strasse 100, 14109 Berlin, Germany.

magnetic ordering with an associated spontaneous magnetization can be observed. Therefore, these compounds constitute a possible pathway to molecular magnetic materials [5–7].

Ferromagnetic coupling in bimetallic chains is observed only in a few cases. The first example was $Mn^{III}Cu^{II}(dmg)_2(H_2O)_2(CH_3CO_2)$, with dmg = dimethylglyoximato, the structure of which, however, was only postulated from EXAFS and XANES studies [8]. The first structurally fully characterized example was $Mn^{II}Ni^{II}(NO_2)_4(en)_2$, reported recently by Kahn *et al* [9]. This compound crystallizes in the orthorhombic structure, space group $Pccn$, with $a = 14.675$ Å, $b = 7.774$ Å and $c = 12.401$ Å at 20 K [10]. As depicted in figure 1, the Mn and Ni ions are linked by NO_2^- ligands forming equally spaced chains in which the two transition metal atom types alternate. The intrachain Mn–Ni distance is equal to 4.79 Å, while the shortest interchain metal–metal distance is significantly larger, namely 5.64 Å (Mn–Ni).

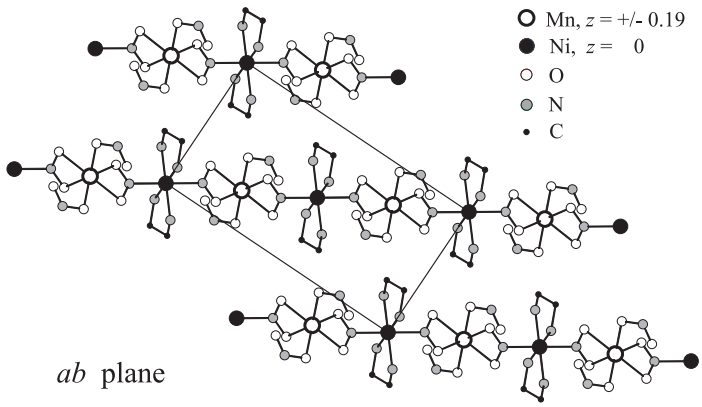

Figure 1. One sheet of the structure of $MnNi(NO_2)_4(en)_2$ showing the equally spaced chains of alternating Mn and Ni ions, running along one *ab* diagonal. In the second sheet of atoms, located at $(z + \frac{1}{2})$, the Mn–Ni chains run along the other *ab* diagonal. In the magnetically ordered phase (see text) all Mn and Ni magnetic moments in one sheet are oriented parallel to each other and antiparallel to the moments in neighbouring sheets. The moment orientation is parallel to *c*, i.e. perpendicular to the paper plane. For clarity, the hydrogen atoms are omitted.

As a spin 1 ion, the Ni^{II} usually exhibits pronounced quantum effects, while the Mn^{II} (spin 5/2) can be treated as (almost) classical spin. In this sense, $MnNi(NO_2)_4(en)_2$ can be regarded as an interesting system of alternating quantum and classical spins.

The magnetic properties of a polycrystalline sample of $MnNi(NO_2)_4(en)_2$ pointed to a dominant ferromagnetic intrachain interaction between Mn and Ni ions ($J/k_B = 1.9$ K) mediated by the NO_2^- ligands [9]. The ferromagnetic nature of the intrachain coupling was evident from the fact that the product of the magnetic susceptibility and the temperature, χT, was larger than the value expected for isolated Mn and Ni spins and increased continuously at decreasing temperatures in the full temperature range 3–300 K. No minimum in the temperature dependence of χT was observed, which would be characteristic for antiferromagnetic intrachain interactions resulting in ferrimagnetic chain behaviour [1].

Below 2.35 K the compound was observed to exhibit long-range antiferromagnetic ordering due to weak interchain interactions. The ordered state was suppressed by relatively small magnetic fields. At 2 K the corresponding metamagnetic transition was observed at a critical field of $H_c = 1.2$ kOe. Polarized neutron diffraction studies in a large applied magnetic field confirmed the parallel spin orientation on the Mn and Ni ions within the chains [10].

In this report we present single crystal magnetization and heat capacity data that give

further insight into the magnetic behaviour of $MnNi(NO_2)_4(en)_2$. In addition, the magnetically ordered structure is determined by neutron diffraction. Very few single crystal magnetization studies of bimetallic chains have been published to date [3] and we are not aware of any heat capacity study or magnetic structure determination by neutron diffraction on other bimetallic chains.

2. Experiment

Single crystals of the title compound have been grown as described in [9]. The crystals show well defined faces and the principal axes can be identified easily.

Magnetization measurements were carried out on a single crystal of about 4 mg mass using an MPMS Squid magnetometer (Quantum Design). Measurements were carried out at temperatures between 1.8 and 300 K in varying magnetic fields H up to 55 kOe and for the three principal crystallographic orientations. The diamagnetic signal from the sample could not be determined because the total temperature independent contribution to the measured magnetization is dominated by the sample holder.

The temperature independent contribution to the magnetization M was determined experimentally by extrapolation of the high temperature data for $1/T \rightarrow 0$ and subtracted from the data. This contribution is small (10^{-3} of the measured values at 20 K) and is dominated by the sample holder (gelatine capsule) signal.

For small applied fields, here $H \leqslant 200$ Oe, the M/H values can be safely assumed to be constant and thus are set equal to the susceptibility. Susceptibility and magnetization values are given per formula unit.

A small impurity contribution was observed below around 40 K that could be minimized by cooling the sample in zero field. This contribution is presumably due to some manganese oxide contamination. For the magnetization data presented in the following this contribution is negligible.

Heat capacity was measured using an Oxford Instrument MagLab calorimeter with ^{3}He refrigerator on a single crystal of about 4 mg mass. The crystal was attached to the sapphire chip, which is the central part of the calorimeter, using a small amount of a grease containing alumina powder (Wakefield 120-2). The temperature dependence of the specific heat was measured in the range 0.4–15 K.

Single-crystal neutron diffraction has been carried out at the Berlin Neutron Scattering Centre (BENSC) at the Hahn–Meitner Institute using the diffractometers E4 and E6. The latter is equipped with a multichannel detector, covering a range of scattering angles of 20°. Neutron wavelengths of 2.441 Å and 2.448 Å, respectively, were used. For part of the experiments, the sample was cooled in an Orange cryostat. For the field dependent measurements the cryomagnet HM2 was used, supplying a horizontal magnetic field. The magnetic field direction was varied by a vertical rotation of the sample. The analysis of the diffraction data was carried out using GSAS [11].

3. Susceptibility and magnetization

Figure 2 shows the temperature dependence of the susceptibility χ and of the product χT for the three principal crystallographic orientations. The general behaviour is similar to the one reported for a polycrystalline sample [9]. For $T > 3$ K, the average value of χT decreases continuously with increasing temperature and approaches asymptotically constant values. As already mentioned above, such a behaviour is usually interpreted as the signature of dominant

ferromagnetic exchange interactions. We find χT values at room temperature of 5.85, 5.92 and 5.70 emu K mol^{-1} for $H \parallel a$, b and c, respectively. These values are slightly larger than the one expected for isolated Mn and Ni spins, $C = 5.63$ emu K mol^{-1}, using the g-factors of the Ni and Mn ions, $g_{Ni} = 2.24$, $g_{Mn} = 2$ [9].

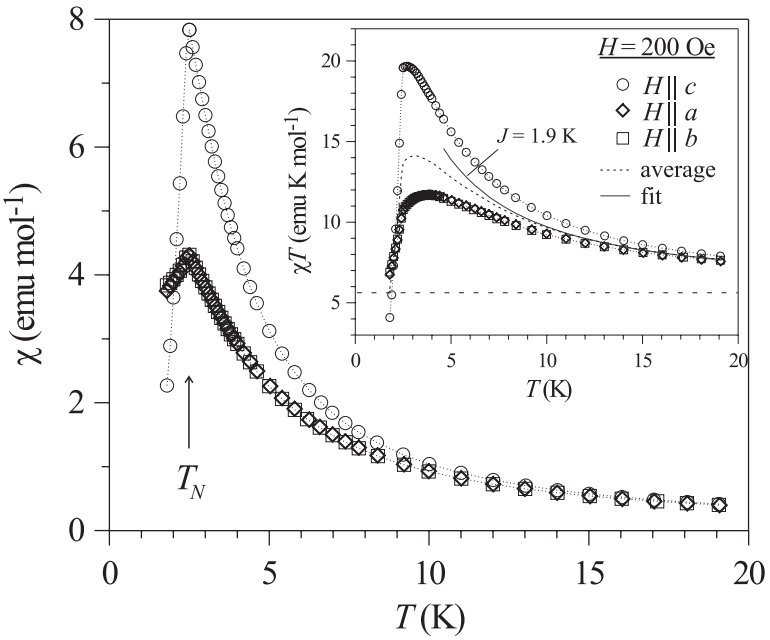

Figure 2. Temperature dependence of the susceptibility χ (main plot) and of the product χT (inset) for the three principal orientations, measured in an applied field of 200 Oe. Steep drops of χ below 2.45 K mark the transition to a long-range antiferromagnetically ordered state. The dotted curves through the data points are guides to the eye. The horizontal dashed line in the inset depicts the χT value expected for a system of non-interacting Mn^{II} and Ni^{II} ions. The deviation of the measured curve to larger values is the signature of dominant ferromagnetic exchange interactions. The dashed curve is the polycrystalline average of the single-crystal data. The solid curve is a model fit to this average (see text). The deviation of the theoretical curve from the data at $T < 10$ K is associated with the zero-field splitting of the Mn^{II} energy levels and the onset of interchain antiferromagnetic interactions.

The rapid drop of the susceptibility below $T_N = 2.45$ K is associated with long-range *antiferromagnetic* ordering. The value of T_N observed in the single crystal is slightly larger than for the polycrystalline sample.

The central new information of the single-crystal data is the presence of a pronounced easy axis anisotropy of the susceptibility at low T. The susceptibility is significantly larger for $H \parallel c$ than for the two perpendicular orientations $H \parallel a$ and $H \parallel b$. We associate this anisotropy with the zero-field splitting due to the spin–orbit coupling. Since, in the present case, the effect of the zero-field splitting on the susceptibility is of similar magnitude as the ferromagnetic exchange interaction (see figure 2), the evaluation of the latter from the data is difficult. The most reliable value can be obtained from the polycrystalline average χ_{av} of the susceptibility although, at low T, it is also affected by the zero-field splitting. In [9], the susceptibility data on a polycrystalline sample have been quantitatively interpreted using a model in which the Mn spin $S_{Mn} = 5/2$ is treated as a classical spin and $S_{Ni} = 1$ is treated as a quantum spin [4]. The intrachain interaction was described by the Hamiltonian $\boldsymbol{H} = -J \sum_j S_{Mn,j} \vec{S}_{Ni,j}$, resulting

in a value for the magnetic exchange constant of $J/k_B = 1.9$ K. It was observed that this model is valid only in the range $T > 10$ K. The corresponding analysis of the single-crystal data confirms this analysis, as shown in figure 2. The deviation of the theoretical curve from the data at $T < 10$ K is associated with the zero-field splitting and the onset of interchain antiferromagnetic interactions. For further discussion of the anisotropy, see section 6.

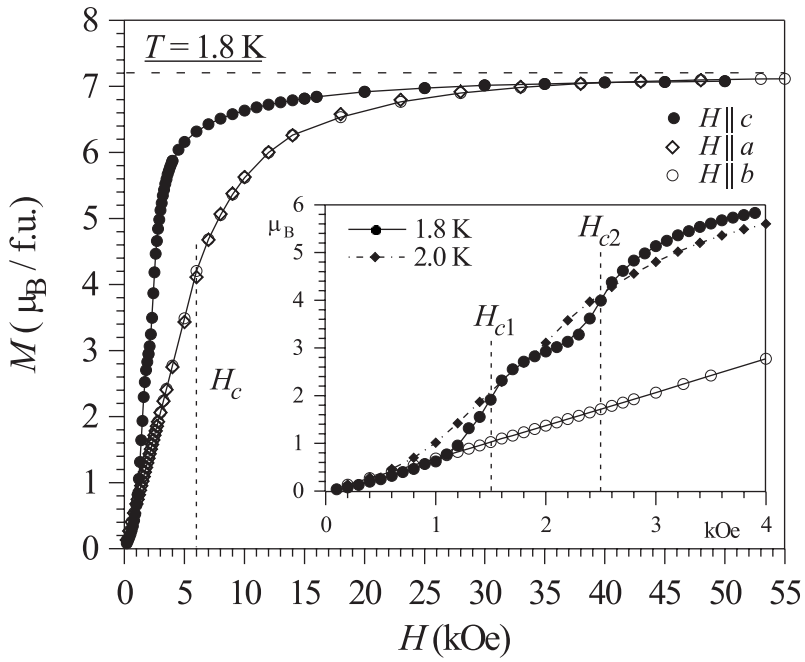

Figure 3. Field dependence of the magnetization for the three principal orientations at 1.8 K. For all curves, every second data point was measured on increasing field, while the other points were measured on decreasing field. No hysteresis is observed. Inset: blow-up of the low-field region. Field dependent transitions are marked by dashed vertical lines.

Figure 3 shows the field dependence of the magnetization at $T = 1.8$ K for the three principal orientations. For high magnetic fields the induced magnetic moments reach a saturation value of about 7.2 μ_B for all field orientations. This value is close to the value expected if all the Mn and Ni moments are oriented along the field direction. For lower fields the magnetization curves depend strongly on the field direction. For $H \parallel c$ a metamagnetic transition is observed that proceeds in two steps (see the inset of figure 3), with $H_{c1} = 1.5$ kOe and $H_{c2} = 2.5$ kOe, defined as the H values for which the steepest slopes of the $M(H)$ curves are observed. In contrast, at 2 K (dashed–dotted curve in figure 3) only one field dependent transition is observed, similar to the behaviour reported for the polycrystalline sample [9]. The plateau region at 1.8 K is presumably associated with the familiar spin flop state at the intermediate field values $H_{c1} < H < H_{c2}$, which is discussed in more detail in section 6. For the $H \perp c$ the induced moment increases less steeply with increasing field. A change of slope of the $M(H)$ curve marks the suppression of the antiferromagnetic ordering at fields larger than 6 kOe for this orientation.

Figure 4 shows the temperature dependence of the magnetization for $H \parallel c$ for different field values. The antiferromagnetic transition is shifted continuously to lower temperatures and drops below the lowest achievable temperature, 1.8 K, at a critical field of 2.5 kOe for

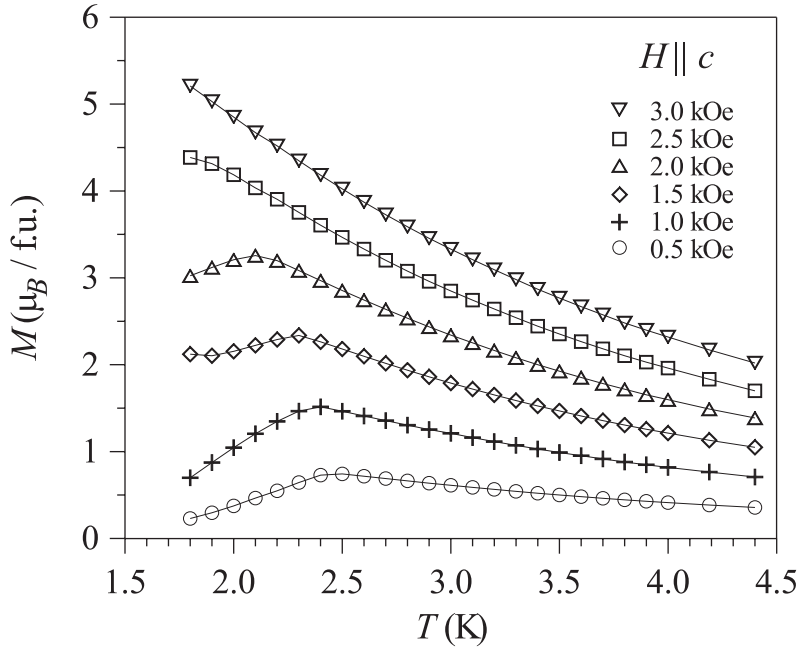

Figure 4. Temperature dependence of the magnetization for different values of the applied magnetic field $H \parallel c$ illustrating the shift of the antiferromagnetic transition.

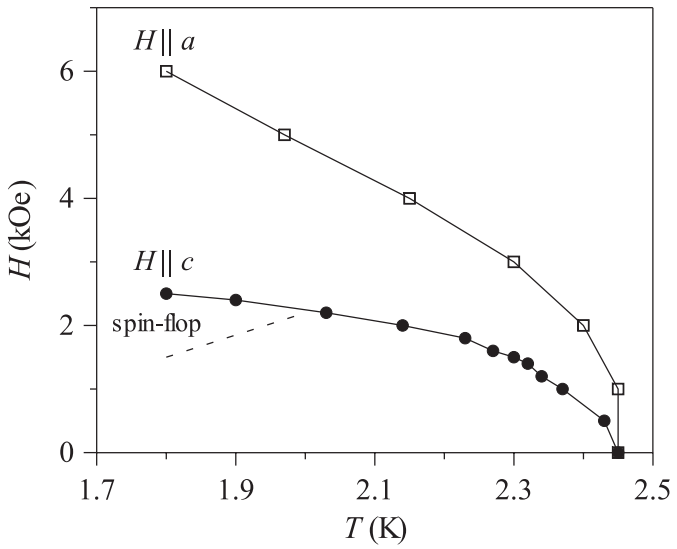

Figure 5. Phase diagram for $MnNi(NO_2)_4(en)_2$ derived from the magnetization data.

$H \parallel c$. A similar data set for $H \perp c$ (not shown) gives a critical field of 6 kOe, consistent with the magnetization data of figure 3. From these data a preliminary phase diagram can be derived that is shown in figure 5.

4. Heat capacity

Figure 6 shows the temperature dependence of the specific heat c and of the entropy, in zero magnetic field. The antiferromagnetic transition is marked by a pronounced λ-type anomaly that peaks at 2.4 K.

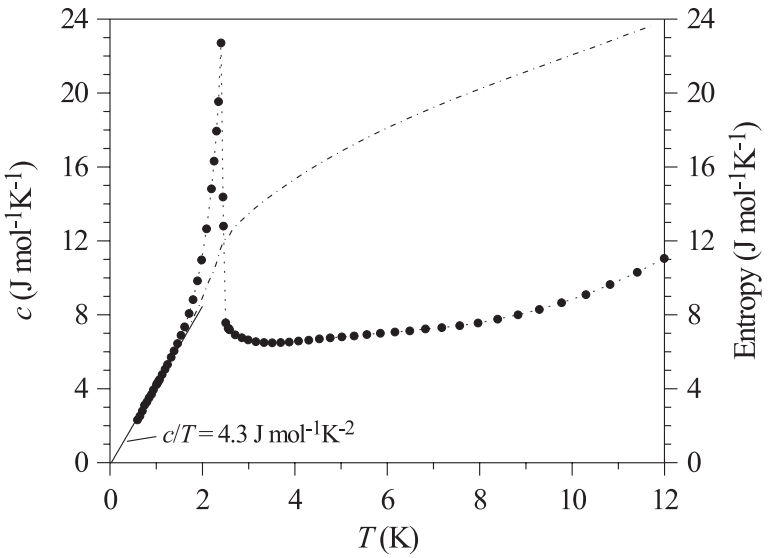

Figure 6. Temperature dependence of the specific heat c (circles) and of the entropy (dashed curve) in zero magnetic field. The solid line is a guide to the eye. The antiferromagnetic transition is marked by a pronounced λ-type anomaly that peaks at 2.4 K.

Below 1.5 K, the specific heat is practically proportional to T, with a ratio c/T of 4.3 J mol^{-1} K^{-2}. The linear extrapolation to $T = 0$ is used to estimate the entropy at 0.5 K. As discussed in more detail in section 6, this interesting T-linear behaviour in the ordered ground state may be related to the specific magnetic structure of $MnNi(NO_2)_4(en)_2$ determined by neutron diffraction (see section 5).

The entropy reaches a value of 11.85 J mol^{-1} K^{-1} at T_N. This is roughly 50% of the full value $R \ln 3 + R \ln 6 = 2.89R = 24.03$ J mol^{-1} K^{-1} expected for the sum of the magnetic entropies of the Ni ($S = 1$) and the Mn ($S = 5/2$) ions. The temperature dependence of c/T suggests that above T_N there is still a significant magnetic contribution to the specific heat. This behaviour points to short-range ordering effects associated with the ferromagnetic intrachain interaction. The full magnetic entropy is reached at about 12 K.

5. Neutron diffraction

The intensity of many Bragg reflections was measured in the three scattering planes ($hk0$), ($h0l$), ($0kl$) by single-crystal neutron diffraction. Since the sample was small and not deuterated, the data are of limited quality due to relatively large background from hydrogen and air scattering. The available data, however, allow for the qualitative determination of the magnetically ordered structure and an estimate of the ordered magnetic moments.

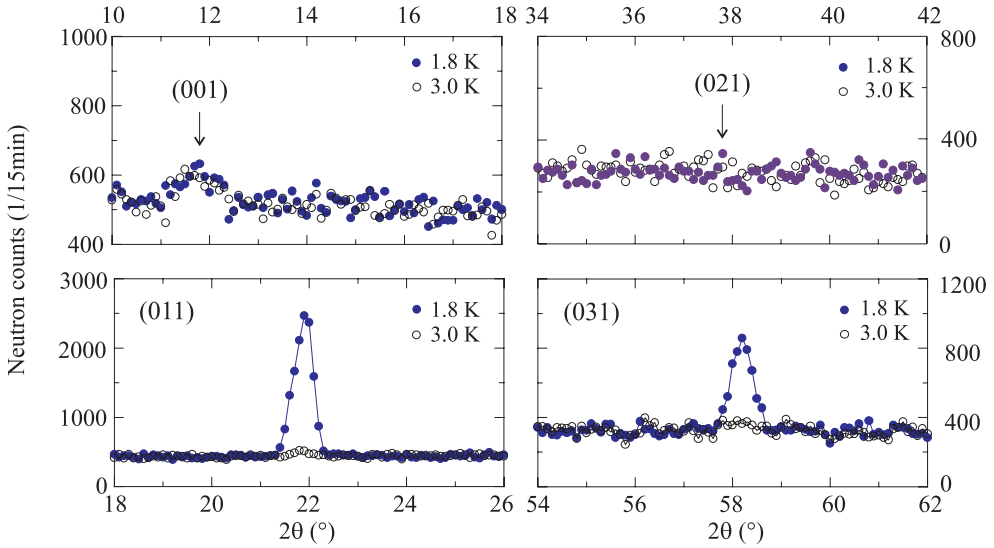

Figure 7. Comparison of Bragg reflections at different positions in reciprocal space below and above $T_N = 2.45$ K. The data were recorded by ω scans at fixed 2θ position of the 20° multichannel detector.

By comparing the intensities of the Bragg reflections at various temperatures, several reflections of magnetic origin were identified that could be indexed on the basis of the crystallographic unit cell, e.g. (110), (310), (101), (301), (011), (031). Figure 7 shows some reflections in the $(0kl)$ plane as examples.

The fact that h, k and l are integer for all magnetic reflections shows that the magnetic and the crystallographic unit cells are identical. Hence, neighbouring Mn–Ni chains in the same sheet (see figure 1) show identical spin arrangements. For an overall antiferromagnetic structure, the Mn–Ni chains of the second sheet have to have an antiparallel spin alignment relative to that of the first sheet. This is consistent with the observed selection rule $l = 2n + 1$ for the magnetic reflections $(h0l)$ and $(0kl)$.

The rule $h + k = 2n$ for the $(hk0)$ reflections shows that within the chains, the metal ions of the same type—which are related by the translation $(1/2, 1/2, z)$—have parallel spin alignment. With this information the spin arrangement within the Mn and Ni sublattices is already determined. It can be described in the magnetic space group $Pccn$, which is identical to the crystallographic one. For this symmetry, the Mn moment orientation is confined to the c axis, consistent with the fact that no magnetic intensity was observed for $(00l)$ positions (see figure 7) and in agreement with the single-crystal susceptibility data.

The relative alignment of Mn and Ni sublattices is not determined by the above-mentioned rules. From the susceptibility data we expect a ferromagnetic alignment. Table 1 shows a list of the ratios of the observed magnetic and selected nuclear Bragg intensities. The magnetic moments of the Mn and Ni ions have been refined on the basis of the structural parameters at 20 K determined by Gillon *et al* [10] and of the proposed magnetic structure.

The fit indeed is consistent with a ferromagnetic alignment of the Mn and Ni magnetic moments within the chains and gives a value for the ordered moment of roughly 90% of the expected full moment of 7 μ_B at 1.8 K. A ferrimagnetic alignment of Mn and Ni moments can be ruled out, since it would lead to significant magnetic Bragg intensity, e.g. at positions (021) and (201), in contrast to the observation.

Table 1. Comparison of measured and calculated ratios of magnetic and selected nuclear Bragg intensities at 1.8 K. The assumed magnetic structures are described in the text. The magnetic moments are oriented along the c axis. The observation of more magnetic reflections of type $(hk0)$ was inhibited by strong nuclear Bragg reflections at the same positions.

(hkl)	I_{magn}/I_{nucl} observed	I_{magn}/I_{nucl} calculated 'ferro' chains: $\mu_{Mn} = 4.70(20)\ \mu_B$ $\mu_{Ni} = 1.65(20)\ \mu_B$	I_{magn}/I_{nucl} calculated 'ferri' chains: $\mu_{Mn} = 4.70\ \mu_B$ $\mu_{Ni} = -1.65\ \mu_B$
	$I/I(110)$	$I/I(110)$	$I/I(110)$
(110)	0.072(6)	0.074	=[a]
(310)	0.042(2)	0.041	=
	$I/I(202)$	$I/I(202)$	$I/I(202)$
(101)	0.059(5)	0.063	=
(201)	<0.005	0.000 02	0.041
(301)	0.030(4)	0.050	=
	$I/I(022)$	$I/I(022)$	$I/I(022)$
(011)	0.141(6)	0.131	=
(021)	<0.005	0.0001	0.049
(031)	0.032(3)	0.039	=
(013)	<0.005	0.004	=

[a] '=' same value as for 'ferro' chains.

We conclude that, in the magnetically ordered state, all Mn and Ni magnetic moments in one sheet of atoms (see figure 1) are oriented parallel to each other and antiparallel to the moments in neighbouring sheets.

The field dependent transitions observed in the magnetization data were further studied by measuring the magnetic field dependence of the intensity of several magnetic reflections at 1.8 and 2.1 K. For $H \parallel c$ at 1.8 K a two-step behaviour was found for the Bragg intensity of the reflection (011), see figure 8. Very similar curves were observed for the (031) and (101) reflections. For all these reflections, the Bragg intensity exhibits a plateau region between 1.7 kOe and 2.2 kOe and vanishing intensity at the metamagnetic transition field 2.6 kOe. The plateau intensity is about one quarter of that observed at zero magnetic field. At 2.1 K, no plateau is observed but the magnetic intensity vanishes continuously with increasing field. Also for $H \perp c$ the Bragg intensities are reduced continuously with increasing magnetic field, vanishing at the transition field of 6 kOe at 1.8 K (not shown). This overall behaviour is consistent with the one observed in the single-crystal magnetization (see figure 3).

The temperature dependence of the magnetic Bragg intensity was measured for several reflections and observed to vanish continuously at T_N (see the inset in figure 8).

6. Discussion

In the present study, several interesting features of $MnNi(NO_2)_4(en)_2$ were observed, namely the magnetic anisotropy with c as the easy axis, the two-step metamagnetic transition for $H \parallel c$, and the short-range ordering effect above T_N. Moreover, the magnetically ordered structure could be determined.

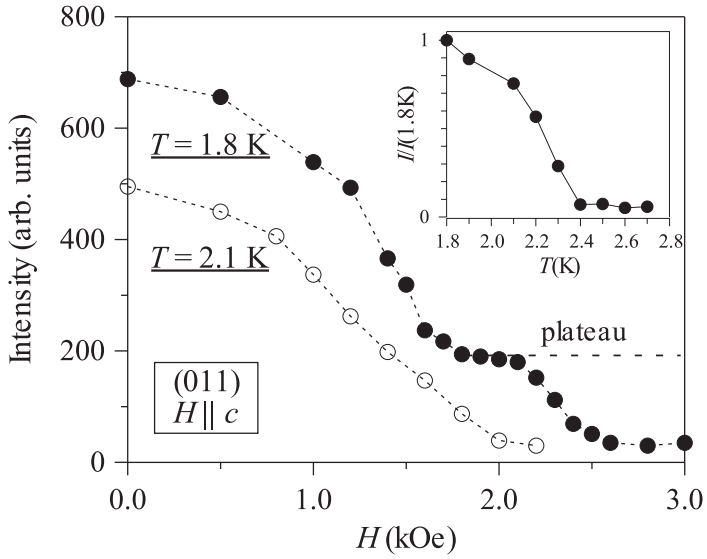

Figure 8. Field dependence of the magnetic Bragg intensity of the (011) reflection at 1.8 K (full circles) and 2.1 K (open circles) for $H \parallel c$. Inset: temperature dependence of the Bragg intensity, normalized to 1.8 K.

6.1. Anisotropy and spin-flop transition

The source of the magnetic anisotropy is most likely a single ion anisotropy due to an orbital contribution to the magnetic moment. The structural data measured at 20 K [10] show that the Ni is surrounded by six N ions, four from the ethylenediamine and two of the NO_2^- ions, which form an almost perfect octahedron (Ni–N distances ranging from 2.090 to 2.138 Å). Due to this high local symmetry the anisotropy from the Ni is assumed to be negligible.

The Mn coordination polyhedron, in contrast, is quite unusual with a 6 + 2 coordination, consisting of O atoms with Mn–O distances between 2.200 and 2.413 Å. The arrangement of the O atoms is irregular and can be regarded as a strongly distorted dodecahedron. The only symmetry lies in a twofold axis parallel to c. Since all available data show that the magnetic anisotropy favours the c direction, this suggests that the source of the anisotropy lies in the local environment of the Mn ions.

In order to estimate the magnitude of the zero-field splitting of the Mn^{II} energy levels, we have calculated the relative deviations $(\chi - \chi_{av})/\chi_{av}$ of the single-crystal data from the polycrystalline average. The results are shown in figure 9 and compared with the corresponding values expected for Mn^{II} in an axially distorted octahedral surrounding [5]. The data are well described by this model, assuming a zero-field splitting of $|D|/k_B = 0.45$ K, although the actual local symmetry of the Mn is lower than the that of the idealized distorted octahedron.

The anisotropy is also responsible for the peculiar two-step metamagnetic transition observed in the magnetization and neutron diffraction data for $H \parallel c$. Without anisotropy, below T_N the magnetic moments would align perpendicular to the external field for any finite value of H because this is the state of lowest energy. In the presence of (weak) anisotropy, the moment orientation switches from the easy axis to an orientation perpendicular to the applied field only for fields larger than a critical value H_{c1}. The associated field dependent transition is called spin flop. The spin-flop field H_{c1} is a measure of the anisotropy energy K_1 defined by the difference of the energies for a moment alignment parallel and perpendicular to the easy

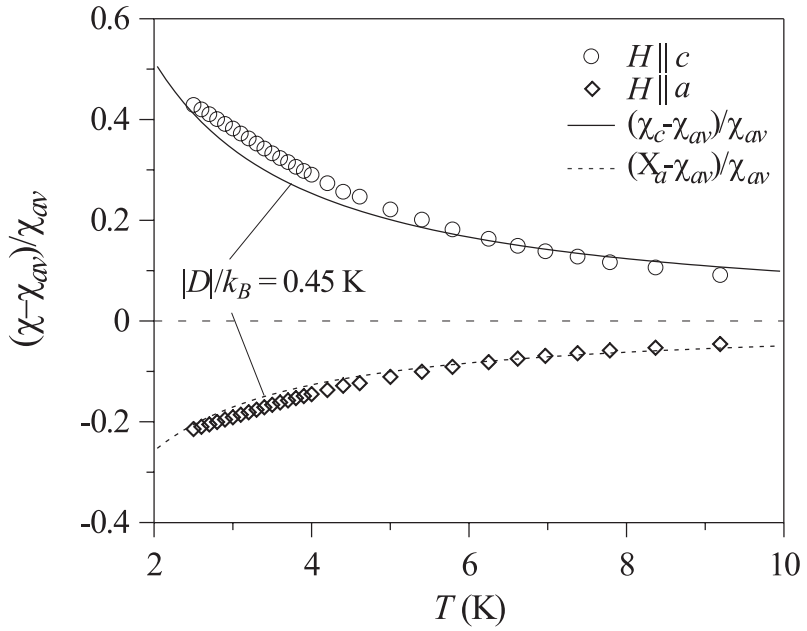

Figure 9. The relative deviations $(\chi - \chi_{av})/\chi_{av}$ observed in the single crystal (data points) and the corresponding values expected for Mn^{II} in an axially distorted octahedral surrounding for $|D|/k_B = 0.45$ K (solid and dashed curves).

direction in zero field. K_1 is given by the simple relation [12]

$$K_1 = \frac{(H_{c1})^2(\chi_a - \chi_c)}{N_A \mu_B}.$$

With $H_{c1} = 1.5$ kOe, $\chi_c = 2.27$ emu mol^{-1} and $\chi_a = 3.75$ emu mol^{-1} at 1.8 K we obtain $K_1 = 3.45$ μeV fu^{-1} or $K_1/k_B = 0.040$ K. When increasing the temperature, the difference $\chi_a - \chi_c$ becomes smaller and finally changes sign above 2 K (see figure 2). Consequently K_1 is reduced and no spin-flop transition is observed at $T \geqslant 2$ K.

To our knowledge, the present work is the first in which a spin-flop transition is reported for a bimetallic chain. We are aware of only one single-crystal magnetization study of another bimetallic chain compound, namely $MnCu(pba)(H_2O)_2$ (pba = 1,3-propylenebis(oxamato) [3], for which the anisotropy ($\chi_a T = 36$ emu K mol^{-1}, $\chi_b T = 7$ emu K mol^{-1} at 2.3 K) is somewhat more pronounced than in $MnNi(NO_2)_4(en)_2$ and the behaviour is more complicated, because all three principal values of χ are different.

6.2. Short-range and long-range ordering

As mentioned already above, the temperature dependence of the specific heat (see figure 6) suggests that above T_N short-range ordering effects associated with the ferromagnetic intrachain interaction play an important role. This interaction appears to result in a *partial* ferromagnetic prealignment of the moments of the single chains above T_N before the long-range ordering takes place on cooling below T_N.

The interchain interaction apparently is dominantly antiferromagnetic. However, within a single *ab* sheet neighbouring chains have a parallel spin alignment in the ordered state. However, this is presumably not due to ferromagnetic interactions between these chains. Let

us assume an antiparallel spin alignment of these chains. Neighbouring chains in the next ab sheet ($z + \frac{1}{2}$) are running along the other diagonal and therefore cross these chains. Then, they would cross chains with parallel and antiparallel moments, which would cause frustration. To avoid such a contradiction, neighbouring chains within a single sheet have to have a ferromagnetic alignment. Actually, this consideration shows that the observed structure is the only possible arrangement consistent with the proposed antiferromagnetic alignment of ferromagnetic chains.

The observed magnetic structure appears to be the key to understanding the T-linear behaviour of the specific heat below 1.5 K. Such a behaviour is, e.g. observed in one-dimensional antiferromagnets. The present magnetic structure is an antiferromagnetic stacking of ferromagnetically coupled sheets. Therefore, the observation of a T-linear specific heat at $T \rightarrow 0$ appears quite natural, assuming that the excitation of antiferromagnetic spin waves along the c axis dominates the thermal behaviour in that temperature range.

7. Conclusion

The present single-crystal magnetization measurements on $MnNi(NO_2)_4(en)_2$ revealed a quite conventional behaviour expected for a system with weak anisotropy, including a spin-flop transition in the ordered state that has not been reported before for any other bimetallic chain compound. The anisotropy is presumably caused by the low symmetry of the Mn environment.

The unusual ferromagnetic interaction between the Mn and Ni ions within the chains does not lead to ferromagnetic long-range order because of the antiferromagnetic interaction between the chains. This causes the long-range antiferromagnetic ordering in $MnNi(NO_2)_4(en)_2$. The ordered structure can be described by an antiferromagnetic stacking of ferromagnetic sheets.

This work showed that single-crystal studies on bimetallic chains can give valuable information on the magnetic properties not available from investigations of polycrystalline samples. However, such studies are rare because most compounds do not grow suitably large single crystals. An increased effort to grow crystals therefore is highly desirable.

Acknowledgments

We thank S Abens and M Meissner for the heat capacity measurements as well as M Hofmann and K Prokeš for experimental support with the neutron diffraction studies.

References

[1] Gleizes A and Verdaguer M 1984 *J. Am. Chem. Soc.* **106** 3727
[2] Pei Y, Verdaguer M, Kahn O, Sletten J and Renard J P 1986 *J. Am. Chem. Soc.* **108** 7428
[3] Kahn O, Pei Y, Verdaguer M, Renard J P and Sletten J 1988 *J. Am. Chem. Soc.* **110** 782
[4] Kahn O, Pei Y, Nakatani N and Journeaux Y 1992 *New J. Chem.* **16** 269
[5] Kahn O 1993 *Molecular Magnetism* (New York: VCH)
[6] Miller J S and Epstein A 1994 *Angew. Chem.* **106** 399
[7] Gatteschi D 1994 *Adv. Mater.* **6** 635
[8] Lloret F, Ruiz R, Julve M, Faus J, Journaux Y, Castro I and Verdaguer M 1992 *Chem. Mater.* **4** 1150
[9] Kahn O, Bakalbassis E, Mathonière C, Hagiwara M, Katsumata K, and Ouahab L 1997 *Inorg. Chem.* **36** 1530
[10] Gillon B, Mathonière C, Kahn O, Ruiz E, Alvarez S and Cousson A, to be published
[11] Larson A C and van Dreele R B 1986 *Los Alamos National Laboratory Report* LA-UCR-86-748
[12] Nolting W 1996 *Quantentheorie des Magnetismus* (Stuttgart: Teubner)